Title

Adenosine Triphosphate Release From Influenza-Infected Lungs Enhances Neutrophil Activation and Promotes Disease Progression

Authors

Ledderose, Carola
Valsami, Eleftheria-Angeliki
Elevado, Mark
et al.

Publication Date

2023-10-06

DOI

10.1093/infdis/jiad442

Peer reviewed

ATP release from influenza-infected lungs enhances neutrophil activation and promotes disease progression

Carola Ledderose[1,2], Eleftheria-Angeliki Valsami[2], Mark Elevado[2], Wolfgang G. Junger[1,2]

[1]Department of Surgery, University of California, San Diego Health, San Diego, CA, USA

[2]Department of Surgery, Beth Israel Deaconess Medical Center, Harvard Medical School, Boston, MA, USA

Correspondence address: Wolfgang G. Junger, UC San Diego Health, Department of Surgery, 9452 Medical Center Drive, La Jolla, CA 92037, USA; e-mail: wgjunger@health.ucsd.edu

Running Title: Influenza primes neutrophils via ATP

Word count (Background to end of Discussion): 3299

Word count (Abstract): 198

Summary

Influenza infection releases ATP that primes peripheral neutrophils and causes their excessive activation after they infiltrate the lungs. Thus, ATP-induced neutrophil priming may be a therapeutic target to reduce lung tissue damage in severe influenza cases.

ABSTRACT

Background: ATP enhances neutrophil responses, but little is known about the role of ATP in influenza infections.

Methods: We used a mouse influenza model to study if ATP release is associated with neutrophil activation and disease progression.

Results: Influenza infection increased pulmonary ATP levels 5-fold and plasma ATP levels 3-fold over the levels in healthy mice. Adding ATP at those concentrations to blood from healthy mice primed their neutrophils and enhanced CD11b and CD63 expression, CD62L shedding, and reactive oxygen species production in response to formyl peptide receptor (FPR) stimulation. Influenza infection also primed neutrophils *in vivo*, resulting in FPR-induced CD11b expression and CD62L shedding up to 3-times higher than that of uninfected mice. In infected mice, large numbers of neutrophils entered the lungs. These cells were significantly more activated than peripheral neutrophils of infected and pulmonary neutrophils of healthy mice. Plasma ATP levels of infected mice and influenza disease progression corresponded with the numbers and activation level of their pulmonary neutrophils.

Conclusion: Our findings suggest that ATP release from the lungs of infected mice promotes influenza disease progression by priming peripheral neutrophils that become strongly activated and cause pulmonary tissue damage after their recruitment to the lungs.

Key words: influenza, mice, neutrophil priming and activation, purinergic signaling, ATP release

BACKGROUND

Influenza is one of the most widespread respiratory viral diseases [1]. It is associated with significant morbidity and mortality and causes over 5 million hospitalizations and approximately 300,000 deaths worldwide each year [2, 3]. Influenza is particularly fatal in infants, older people, and in patients with chronic pulmonary diseases and other comorbidities [3, 4]. Highly pathogenic and pandemic influenza A virus strains can cause lethal illness even among less vulnerable adult populations [5]. Severe disease often involves a dysregulated immune response that results in pneumonia, acute respiratory distress syndrome (ARDS), and multiple organ dysfunction syndrome (MODS) [6, 7].

The role of polymorphonuclear neutrophils (PMNs) in influenza infections is not clear [8-10]. Some studies have shown that PMNs reduce viral spread, help to resolve inflammation, and prevent secondary bacterial infections that often complicate the treatment of severe influenza cases [9, 11, 12]. Other reports suggest that PMNs contribute to excessive inflammation that promotes pulmonary tissue damage and disease progression following influenza virus infections [13-15].

PMNs are essential for antimicrobial host defense. They rapidly accumulate in the circulation and infiltrate sites of infection by attaching to the endothelial layer of blood vessels and transmigrating into affected tissues. These processes require the upregulation of CD11b on the

cell surface of PMNs and shedding of CD62L (L-selectin) [16, 17]. At the sites of infection, chemotaxis guides PMNs towards microbial invaders that they entrap and kill with a wide arsenal of defensive strategies [18, 19].

Gradient sensing and chemotaxis of PMNs towards bacterial invaders depend on cellular ATP release and autocrine feedback mechanisms that involve purinergic receptors [20]. The family of purinergic receptors comprises seven P2X, eight P2Y, and four P1 receptors that recognize ATP, ADP, adenosine, and related nucleotides [21]. PMNs express primarily the P2Y2 and A2a subtypes [22]. ATP promotes PMN responses via P2Y2 receptors, while the ATP breakdown product adenosine attenuates cell responses via A2a receptor signaling. The orchestrated actions of both purinergic receptor subtypes regulate complex PMN functions including gradient sensing, chemotaxis, and the phagocytosis of invading microorganisms [20, 22, 23].

However, damaged host tissues also release ATP, which acts as a danger signal that promotes inflammation and alters immune responses [24]. High extracellular ATP levels not only disrupt the regulatory mechanisms that PMNs need for host defense [23, 25] but also promote the uncontrolled production and release of cytotoxic mediators that further damage alveolar epithelial-endothelial barriers and contribute to ARDS and MODS [7, 10].

Several studies have shown that viral infections cause ATP release. For example, infections with human immunodeficiency virus, severe acute respiratory syndrome coronavirus 2, vesicular stomatitis virus, and certain influenza virus strains have been shown to cause ATP release that is thought to affect viral entry, viral replication, and inflammation [26-29]. In this study, we

evaluated the hypothesis that influenza infection-induced ATP release contributes to disease progression by promoting dysregulated PMN activation that damages lung tissues.

MATERIALS AND METHODS

Virus preparation

The mouse-adapted influenza virus strain (H1N1) A/Puerto Rico/8-9NMC3/1934 (PR8) was from the BEI Resources Repository (NR-29025; National Institute of Allergy and Infectious Diseases) and kindly provided by Dr. Daniel Lingwood (Ragon Institute, Massachusetts General Hospital, Boston, MA). Virus stocks were propagated in Madin-Darby Canine Kidney (MDCK) cells (ATCC, Manassas, VA), titrated, and their concentrations shown as median tissue culture infectious doses ($TCID_{50}$) following previously described protocols [30].

Mice

All animal experiments were approved by the Institutional Animal Care and Use Committee of Beth Israel Deaconess Medical Center and performed in accordance with National Institutes of Health guidelines for the care and use of laboratory animals. C57BL/6J mice were from Jackson Laboratory (Bar Harbor, ME), housed in groups of 2-5 mice per cage with free access to standard rodent food and water, and maintained at a 12-hour dark/light cycle. Experiments were performed with equal numbers of 8- to 12-week-old male and female mice per group.

Influenza infection model

Mice were lightly anesthetized with isoflurane and intranasally infected with indicated doses of influenza virus preparations in sterile phosphate buffered saline (PBS) using 20 µl per nostril.

Control animals received equal volumes of PBS. Buprenorphine SR-LAB (1.2 mg/kg; ZooPharm, Laramie, WY) administered subcutaneously at the time of infection was used for pain control. Animals were assessed at least twice daily and clinical signs of illness and body weight were recorded.

Blood collection

At indicated time points, mice were anesthetized and exsanguinated by cardiac puncture. Blood was drawn from the right ventricle using a 23-gauge needle and a 1-ml syringe wetted with sodium heparin. For the analysis of plasma ATP concentrations, aliquots of blood were immediately chilled in an ice water bath. The remaining blood was kept at room temperature and analyzed by flow cytometry within 1 h after blood collection.

Analysis of plasma ATP levels with high performance liquid chromatography (HPLC)

Plasma ATP concentrations were determined as previously described [31]. Briefly, plasma was prepared from chilled heparinized blood samples, stabilized with perchloric acid (MilliporeSigma, St. Louis, MO), and spiked with the internal standard adenosine 5'-(α,β-methylene)-diphosphate (AMPCP; MilliporeSigma). Fluorescent 1,N^6-etheno-derivatives of ATP and AMPCP were generated, pre-purified by solid phase extraction, and concentrated as described [31]. Samples were analyzed with an Agilent 1260 Infinity HPLC system (Agilent, Santa Clara, CA). Plasma ATP concentrations were calculated based on a standard mixture of ATP and AMPCP processed and analyzed in parallel.

PMN blood counts

Heparinized blood samples were labeled with anti-CD11b APC (clone M1/70) and anti-Ly6G Brilliant Violet 421 (clone 1A8) antibodies (BioLegend, San Diego, CA) for 20 min on ice, treated with RBC Lysis/Fixation buffer (BioLegend), and the numbers of PMNs (CD11b/Ly6G double-positive cells) were determined by flow cytometry (NovoCyte 3000, Agilent, Santa Clara, CA).

Assessment of PMN activation levels

CD11b expression and CD62L shedding were measured to assess PMN activation states. Heparinized blood samples were stained with anti-Ly6G Brilliant Violet 421, anti-CD11b APC, and anti-CD62L FITC (clone MEL-14) antibodies (BioLegend), treated with RBC Lysis/Fixation buffer, and analyzed by flow cytometry. Fluorescence-minus-one controls (FMO) were used to define positive staining. CD11b positive ($CD11b^+$) PMNs were defined as PMNs displaying CD11b fluorescence higher than unstimulated PMNs of healthy controls.

Assessing the priming state of PMNs

Priming of PMNs exposed to different concentrations of ATP or viral infection was assessed by measuring their response to *in vitro* stimulation with the formyl peptide receptor (FPR) agonist WKYMVm (W-peptide; Tocris Bioscience, Minneapolis, MN) compared to unprimed cells. Specifically, we analyzed shedding of CD62L, the upregulation of CD11b or the degranulation marker CD63, and the production of reactive oxygen species (ROS) as previously described [32]. Blood from healthy mice was treated for 1 min with ATP (MilliporeSigma). Then, these samples or blood from virus-infected mice were stimulated with 50 nM W-peptide for 10 min at 37°C. For the assessment of ROS production, blood samples were stained for 5 min with 100 µM

dihydrorhodamine-123 (DHR; Invitrogen, Carlsbad, CA), treated or not with ATP, and stimulated with 100 nM W-peptide for 20 min. The reactions were stopped on ice, samples stained with anti-Ly6G Brilliant Violet 421, anti-CD11b APC, anti-CD62L FITC, and anti-CD63 PE (clone NVG-2, BioLegend) antibodies, treated with RBC Lysis/Fixation buffer, and analyzed by flow cytometry.

Analysis of PMN numbers in bronchoalveolar lavage fluids

Immediately after exsanguination, a blunt 23-gauge needle was inserted into the trachea and bronchoalveolar lavage fluid (BALF) was collected by flushing the lungs four times each with 1 ml ice-cold lavage fluid. The first lavage was done with sterile saline followed by three additional lavages with saline containing 0.1% bovine serum albumin (BSA). BALF samples were centrifuged at 400 x *g* for 5 min at 0°C. The supernatant of the first lavage was treated with perchloric acid and stored at -80°C for HPLC analysis. Cell pellets from the combined lavage fluids were used to assess total leukocyte counts with a hemocytometer. For differential counting of leukocytes, cells were stained with a Hema 3^{TM} staining kit (Fisher Scientific, Waltham, MA) and 200 cells per sample were analyzed.

Analysis of PMN activation in the lungs

CD11b expression levels of PMNs in BALF samples were determined as a measure of the activation of PMNs recruited into the lungs. BALF samples were adjusted to a cell concentration of 5-10 x 10^5 cells/ml, stained with anti-CD11b and anti-Ly6G antibodies, washed with PBS/1% BSA, and analyzed by flow cytometry. PMNs were identified as cells that are positive for

CD11b and Ly6G. Cellular debris was analyzed based on forward and side scatter properties and CD11b and Ly6G staining to estimate the degree of PMN deterioration following degranulation.

Analysis of ATP levels in bronchoalveolar lavage fluids

BALF samples stabilized with perchloric acid and stored at -80°C were thawed on ice, spiked with AMPCP, and analyzed by HPLC as described above. Alveolar ATP concentrations were estimated based on the approximate alveolar fluid lining volume of 6 µl reported for mouse lungs [33].

Statistical analyses

Differences between two groups were tested for statistical significance using a two-tailed t test or Mann-Whitney test for normally and not normally distributed data, respectively. One-way ANOVA followed by Holm-Sidak's test was used for multiple group comparisons when data were normally distributed. Kruskal-Wallis and post-hoc Dunn's tests were used when data were not normally distributed. Correlations between parameters were assessed by Pearson's test. Four-parameter logistic regression curve fittings and calculations of half maximal effective concentrations (EC_{50}) as well as all other statistical analyses were done with SigmaPlot 12.5 software (Systat Software Inc., San Jose, CA). Differences were considered statistically significant at $p<0.05$.

RESULTS

Influenza infection of mice causes PMN accumulation in the lungs

Infection of mice with the mouse-adapted influenza A virus strain PR8 at a dose of 500 $TCID_{50}$

or higher led to a significant body weight loss within 3 days (Figure 1A). Significant weight loss was evident within 2 days after infection with a dose of 1,000 $TCID_{50}$, resulting in an average drop in body weight of about 20% within 4 days (Figure 1B). This dose also caused a 10-fold increase in the number of leukocytes in the BALF 3 days after infection. The numbers of PMNs rose from about 80 cells in control animals to 1.4 x 10^6 cells in infected mice (Figure 1C). In addition, the average number of PMNs in blood nearly doubled from 140 ± 22 per µl in controls to 266 ± 37 per µl in infected animals (Figure 1C). These results are consistent with previous reports that PMN influx into the lungs contributes to the pathogenesis of influenza [13, 14, 34].

ATP release correlates with disease progression

Next, we studied whether influenza infection alters extracellular ATP levels. Mice were infected with 500-1,500 $TCID_{50}$ of PR8 virus and plasma ATP concentrations were determined 3 days later. We found dose-dependent increases in plasma ATP levels (Figure 2A). At the highest viral load, plasma ATP levels reached an average of about 170 nM, which was 3-times higher than in healthy controls. ATP concentrations in moderately sick animals doubled from a baseline value of 60 ± 7 nM to 128 ± 15 nM 3 days after infection (Figure 2B). ATP levels correlated with body weight loss (Figure 2C), which is a reliable indicator of disease progression in influenza-infected mice [35]. In summary, these data show that ATP release is associated with influenza infection and disease progression.

ATP released in the lungs of influenza-infected mice spreads throughout their circulation

A source of ATP in the plasma of infected mice is the release from damaged tissue in the lungs. As shown in Figure 3A, lung ATP levels 3 days after infection with 1,000 $TCID_{50}$ were with

5,650 ± 880 nM over 5-times higher than in healthy controls (1,020 ± 250 nM). ATP plasma levels in these animals were about 3-times higher (156 ± 14 nM) when compared to healthy mice (59 ± 7 nM; Figure 3A). The ATP concentrations in the alveolar space correlated significantly with plasma ATP levels (Figure 3B), suggesting that ATP leaking from damaged lung tissue spreads throughout the circulatory system of infected mice.

Extracellular ATP dose-dependently primes mouse PMNs

The transition of PMNs from a quiescent to a fully activated state involves PMN priming, which readies PMNs for robust functional responses to a variety of subsequent stimuli [36]. Extracellular ATP is known to prime human PMN responses to formyl peptide receptor (FPR) stimulation [37, 38]. We studied whether ATP has similar priming effects on mouse PMNs. Adding ATP to blood samples of healthy mice dose-dependently augmented CD11b expression on the surface of PMNs in response to FPR stimulation with the agonist W-peptide (Figure 4A). ATP levels as low as 100 nM primed CD11b responses by about 15-fold with an EC_{50} value of 140 nM ATP (Figure 4A-B). ATP also markedly increased the shedding of CD62L in response to FPR stimulation with an EC_{50} value of 114 nM (Figure 4C-D). CD11b expression and CD62L shedding are both early and sensitive markers of PMN activation and aid the transendothelial migration of PMNs to sites of infection [16, 17]. ATP also primed PMN degranulation and oxidative burst as seen by increased CD63 expression and ROS production (Supplementary Figure 1).

Influenza infection primes circulating PMNs

Taken together, the findings above suggest that the increase in extracellular ATP enhances the

247 priming state of PMNs following influenza infection. Indeed, we found that PMNs of influenza-
248 infected mice showed significantly stronger CD11b expression responses to FPR stimulation
249 when compared to healthy controls (Figure 5A). Similarly, FPR-induced CD62L shedding was
250 significantly higher when compared to PMNs of healthy mice (Figure 5B). These priming effects
251 on PMNs gradually increased over time after viral infection (Figure 5C-D). Taken together with
252 the time-dependent increase in plasma ATP levels in infected mice (Figure 2B) and the priming
253 effect of ATP on mouse PMNs (Figure 4), these results suggest that ATP that is released from
254 damaged lungs drives PMN priming in influenza-infected mice.
255
256 **PMNs are activated in the lungs but not in the circulation of influenza-infected mice**
257 As shown above, influenza caused a robust increase in the priming state of peripheral PMNs,
258 making them significantly more responsive to FPR stimulation (Figure 5). However, the
259 activation state of PMNs in the blood was not markedly increased and CD11b expression did not
260 differ between infected and healthy animals (Figure 6A). The same was true for CD62L
261 shedding (Figure 5B). However, the PMNs that infiltrated the lungs of infected mice showed
262 strong CD11b expression, which was significantly higher than that of peripheral PMNs and of
263 PMNs in the lungs of healthy mice (Figure 6B). Taken together, these findings show that
264 influenza infection primes peripheral PMNs, but that these cells become activated only after their
265 recruitment into the lungs, possibly by local release of mediators that stimulate FPR or other
266 danger-sensing receptors of PMNs.
267
268 **Activation of pulmonary PMNs correlates with disease progression**
269 Activated PMNs degranulate and release their arsenal of cytotoxic mediators to kill invading

microorganisms but this can also cause substantial collateral damage to host tissues [39]. We found that the percentage of PMNs infiltrating the lungs correlated with body weight loss of influenza-infected mice (Figure 7A). In addition, expression levels of the PMN activation marker CD11b on cellular debris found in the lungs of infected animals closely correlated with body weight loss, suggesting that PMN degranulation promotes disease progression (Figure 7B). Furthermore, high CD11b expression levels on Ly6G-positive cellular debris derived from PMNs correlated with increased plasma ATP concentrations (Figure 7C). Taken together, these findings suggest that the peripheral priming of PMNs by ATP followed by their influx and activation in the lungs leads to PMN degranulation that damages lung tissue and defines disease progression in influenza virus infection (Figure 7D).

DISCUSSION

Influenza remains a leading cause of morbidity and mortality worldwide [2]. In severe influenza cases, a so-called "cytokine storm," inflammatory tissue damage, and secondary microbial infections culminate in lethal complications such as pneumonia, ARDS, sepsis, and MODS [6, 7]. PMNs are among the first immune cells recruited into influenza-infected lungs where they are thought to fight microbial invaders. However, when dysregulated, PMNs lose their ability to locate and eliminate invading microbes and instead contribute to lung tissue damage through uncontrolled release of ROS, proteinases, and other cytotoxic mediators [10, 13, 15].

We found increased numbers of PMNs in the circulation and the lungs of influenza-infected mice, which was paralleled by an increase in extracellular ATP levels in the alveolar space and plasma. PMNs themselves release ATP to regulate chemotaxis and other defensive effector

functions via complex autocrine feedback mechanisms that involve P2Y2 and adenosine A2a receptors on the cell surface [20, 22, 23, 40, 41]. Uncontrolled accumulation of ATP in the extracellular environment distorts these autocrine feedback mechanisms, resulting in impaired antimicrobial host defenses and uncontrolled release of cytotoxic mediators that cause collateral tissue damage [37, 42, 43].

The accumulation of PMN debris we found in the lungs of infected mice suggests that PMN-mediated lung tissue damage is a main source of the increased extracellular ATP levels in our influenza model. However, other mechanisms may also contribute to the accumulation of extracellular ATP. For example, NLPR3 inflammasome activation involves ATP release and P2X7 receptor stimulation. Previous work has shown reduced PMN infiltration and improved survival of influenza-infected P2X7 receptor-deficient mice when compared to wild-type mice, which supports the notion that NLPR3 inflammasome/P2X7 receptor signaling contributes to PMN dysregulation and influenza disease progression [44].

We found that extracellular ATP concentrations as low as 100 nM were sufficient to prime mouse PMNs and that equivalent ATP levels were readily achieved in the alveolar and plasma compartments of influenza-infected mice. Although circulating PMNs of these mice were strongly primed, only PMNs in the lungs were activated. However, the primed state of the circulating PMNs resulted in significantly enhanced cell activation in response to stimulation with the FPR agonist W-peptide. The primed state of peripheral PMNs increased over time after influenza infection and paralleled the increase in plasma ATP levels. The observation that PMNs are activated only after their recruitment into the lungs indicates that additional stimuli in

316 infected lungs complete the stimulation process that results in full PMN activation. This concept
317 is supported by previous work that has shown that ATP primes PMNs but does not activate these
318 cells in the absence of other stimuli [37, 38].
319
320 The activation of PMNs in the lungs of influenza-infected mice may occur through local stimuli
321 such as pathogen- or danger-associated molecular patterns (PAMPs and DAMPs), which include
322 ligands of Toll-like (TLR), NOD-like (NLR), and formyl peptide receptors (FPR) that are
323 released in inflamed and infected tissues [45, 46]. Along with released ATP, those PAMPs and
324 DAMPs may lead to uncontrolled PMN activation, driving a feed-forward process that
325 culminates in disease progression and the lethal consequences of severe cases of influenza
326 infections (Figure 7D).
327
328 Our findings suggest that extracellular ATP accumulation could be a potential therapeutic target
329 to treat severe influenza cases. Possible therapeutic strategies could include treatments with
330 antagonists of P2Y2 and P2X7 receptors, with ATP-hydrolyzing enzymes such as apyrase, or
331 with other drugs that target ATP release mechanisms [44, 47]. These approaches have yielded
332 encouraging results in mouse models of influenza and other clinical conditions that culminate in
333 ARDS and MODS, including endotoxemia, pancreatitis, and sepsis [25, 47-50].
334
335 A limitation of our study is that the mouse model we used does not fully replicate typical human
336 influenza cases, but rather infections with highly pathogenic influenza strains, which often
337 include secondary bacterial infections [12]. Therapeutic strategies such as the ones mentioned
338 above will be complicated by the fact that removal of extracellular ATP can impair antimicrobial

host defenses, e.g., PMN gradient sensing and chemotaxis that require autocrine purinergic signaling. Effective therapeutic interventions targeting ATP must find a balance between the dual roles of ATP as a regulator and disruptor of PMN functions. Future work will have to evaluate the potential of ATP and purinergic signaling mechanisms as viable therapeutic targets to improve outcome in clinically relevant models of influenza infections.

Conflict of interest: The authors declare no conflicts of interest.

Funding

This study was funded in part by grants from the National Institutes of Health, R35 GM-136429, R01 HD-098363, and R01 GM-116162 (to W.G.J.) and fellowship from the Austrian Marshall Plan Foundation (to M. E.).

REFERENCES

1. Paules C, Subbarao K. Influenza. Lancet **2017**; 390:697-708.
2. Lafond KE, Porter RM, Whaley MJ, et al. Global burden of influenza-associated lower respiratory tract infections and hospitalizations among adults: A systematic review and meta-analysis. PLoS Med **2021**; 18(3):e1003550.
3. Uyeki TM, Hui DS, Zambon M, Wentworth DE, Monto AS. Influenza. Lancet **2022**; 400:693-706.
4. Kunisaki KM, Janoff EN. Influenza in immunosuppressed populations: a review of infection frequency, morbidity, mortality, and vaccine responses. Lancet Infect Dis **2009**; 9:493-504.

5. Taubenberger JK, Morens DM. The pathology of influenza virus infections. Annu Rev Pathol **2008**; 3:499-522.
6. de Jong MD, Simmons CP, Thanh TT, et al. Fatal outcome of human influenza A (H5N1) is associated with high viral load and hypercytokinemia. Nat Med **2006**; 12:1203-07.
7. Short KR, Kroeze EJBV, Fouchier RAM, Kuiken T. Pathogenesis of influenza-induced acute respiratory distress syndrome. Lancet Infect Dis **2014**; 14:57-69.
8. Tumpey TM, García-Sastre A, Taubenberger JK, et al. Pathogenicity of influenza viruses with genes from the 1918 pandemic virus: functional roles of alveolar macrophages and neutrophils in limiting virus replication and mortality in mice. J Virol **2005**; 79:14933-44.
9. Tate MD, Deng YM, Jones JE, Anderson GP, Brooks AG, Reading PC. Neutrophils ameliorate lung injury and the development of severe disease during influenza infection. J Immunol **2009**; 183:7441-50.
10. Narasaraju T, Yang E, Samy RP, et al. Excessive neutrophils and neutrophil extracellular traps contribute to acute lung injury of influenza pneumonitis. Am J Pathol **2011**; 179:199-210.
11. Tate MD, Ioannidis LJ, Croker B, Brown LE, Brooks AG, Reading PC. The role of neutrophils during mild and severe influenza virus infections of mice. PLoS One **2011**; 6(3):e17618.
12. Morens DM, Taubenberger JK, Fauci AS. Predominant role of bacterial pneumonia as a cause of death in pandemic influenza: implications for pandemic influenza preparedness. J Infect Dis **2008**; 198:962-70.

13. Perrone LA, Plowden JK, García-Sastre A, Katz JM, Tumpey TM. H5N1 and 1918 pandemic influenza virus infection results in early and excessive infiltration of macrophages and neutrophils in the lungs of mice. PLoS Pathog **2008**; 4(8):e1000115.
14. Dunning J, Blankley S, Hoang LT, et al. Progression of whole-blood transcriptional signatures from interferon-induced to neutrophil-associated patterns in severe influenza. Nat Immunol **2018**; 19:625-35.
15. Tang BM, Shojaei M, Teoh S, et al. Neutrophils-related host factors associated with severe disease and fatality in patients with influenza infection. Nat Commun **2019**; 10:3422.
16. Rochon YP, Kavanagh TJ, Harlan JM. Analysis of integrin (CD11b/CD18) movement during neutrophil adhesion and migration on endothelial cells. J Microsc **2000**; 197:15-24.
17. Rahman I, Collado Sánchez A, Davies J, et al. L-selectin regulates human neutrophil transendothelial migration. J Cell Sci **2021**; 134:jcs250340.
18. Winterbourn CC, Kettle AJ, Hampton MB. Reactive oxygen species and neutrophil function. Annu Rev Biochem **2016**; 85:765-92.
19. Othman A, Sekheri M, Filep JG. Roles of neutrophil granule proteins in orchestrating inflammation and immunity. FEBS J **2022**; 289:3932-53.
20. Junger WG. Immune cell regulation by autocrine purinergic signalling. Nat Rev Immunol **2011**; 11:201-12.
21. Ralevic V, Burnstock G. Receptors for purines and pyrimidines. Pharmacol Rev **1998**; 50:413-92.

22. Bao Y, Chen Y, Ledderose C, Li L, Junger WG. Pannexin 1 channels link chemoattractant receptor signaling to local excitation and global inhibition responses at the front and back of polarized neutrophils. J Biol Chem **2013**; 288:22650-57.
23. Chen Y, Corriden R, Inoue Y, et al. ATP release guides neutrophil chemotaxis via P2Y2 and A3 receptors. Science **2006**; 314:1792-95.
24. Idzko M, Ferrari D, Eltzschig HK. Nucleotide signalling during inflammation. Nature **2014**; 509:310-17.
25. Li X, Kondo Y, Bao Y, et al. Systemic adenosine triphosphate impairs neutrophil chemotaxis and host defense in sepsis. Crit Care Med **2017**; 45:e97-e104.
26. Velasquez S, Prevedel L, Valdebenito S, et al. Circulating levels of ATP is a biomarker of HIV cognitive impairment. EBioMedicine **2020**; 51:102503.
27. da Silva GB, Manica D, da Silva AP, et al. High levels of extracellular ATP lead to different inflammatory responses in COVID-19 patients according to the severity. J Mol Med (Berl) **2022**; 100:645-63.
28. Zhang C, He H, Wang L, et al. Virus-triggered ATP release limits viral replication through facilitating IFN-β production in a P2X7-dependent manner. J Immunol 2017; 199:1372-81.
29. Wolk KE, Lazarowski ER, Traylor ZP, et al. Influenza A virus inhibits alveolar fluid clearance in BALB/c mice. Am J Respir Crit Care Med **2008**; 178:969-76.
30. Karakus U, Crameri M, Lanz C, Yángüez E. Propagation and titration of influenza viruses. Methods Mol Biol **2018**; 1836:59-88.

31. Ledderose C, Valsami EA, Junger WG. Optimized HPLC method to elucidate the complex purinergic signaling dynamics that regulate ATP, ADP, AMP, and adenosine levels in human blood. Purinergic Signal **2022**; 18:223-39.
32. Ledderose C, Hashiguchi N, Valsami EA, Rusu C, Junger WG. Optimized flow cytometry assays to monitor neutrophil activation in human and mouse whole blood samples. J Immunol Methods **2023**; 512:113403.
33. Icard P, Saumon G. Alveolar sodium and liquid transport in mice. Am J Physiol **1999**; 277: L1232-L8.
34. Brandes M, Klauschen F, Kuchen S, Germain RN. A systems analysis identifies a feedforward inflammatory circuit leading to lethal influenza infection. Cell **2013**; 154:197-212.
35. Trammell RA, Toth LA. Markers for predicting death as an outcome for mice used in infectious disease research. Comp Med **2011**; 61:492-8.
36. Condliffe AM, Kitchen E, Chilvers ER. Neutrophil priming: pathophysiological consequences and underlying mechanisms. Clin Sci (Lond) **1998**; 94:461-71.
37. Kuhns DB, Wright DG, Nath J, Kaplan SS, Basford RE. ATP induces transient elevations of $[Ca^{2+}]_i$ in human neutrophils and primes these cells for enhanced O_2^- generation. Lab Invest **1988**; 58:448-53.
38. Ledderose C, Valsami EA, Newhams M, Elevado MJ, Novak T, Randolph AG, Junger WG. ATP breakdown in plasma of children limits the antimicrobial effectiveness of their neutrophils. Purinergic Signal **2023**; doi: 10.1007/s11302-022-09915-w. [online ahead of print]

448 39. Kruger P, Saffarzadeh M, Weber AN, et al. Neutrophils: Between host defence, immune
449 modulation, and tissue injury. PLoS Pathog **2015**; 11(3),e1004651.
450 40. Chen Y, Yao Y, Sumi Y, et al. Purinergic signaling: a fundamental mechanism in
451 neutrophil activation. Sci Signal **2010**; 3(125):ra45.
452 41. Wang X, Chen D. Purinergic regulation of neutrophil function. Front Immunol **2018**;
453 9:399.
454 42. Seifert R, Wenzel K, Eckstein F, Schultz G. Purine and pyrimidine nucleotides potentiate
455 activation of NADPH oxidase and degranulation by chemotactic peptides and induce
456 aggregation of human neutrophils via G proteins. Eur J Biochem **1989**; 181:277-85.
457 43. Axtell RA, Sandborg RR, Smolen JE, Ward PA, Boxer LA. Exposure of human
458 neutrophils to exogenous nucleotides causes elevation in intracellular calcium,
459 transmembrane calcium fluxes, and an alteration of a cytosolic factor resulting in
460 enhanced superoxide production in response to FMLP and arachidonic acid. Blood **1990**;
461 75:1324‑32.
462 44. Leyva-Grado VH, Ermler ME, Schotsaert M, Gonzalez MG, Gillespie V, Lim JK,
463 García-Sastre A. Contribution of the purinergic receptor P2X7 to development of lung
464 immunopathology during influenza virus infection. mBio **2017**; 8:e00229-17.
465 45. Zhang Q, Raoof M, Chen Y, et al. Circulating mitochondrial DAMPs cause inflammatory
466 responses to injury. Nature **2010**; 464:104-7.
467 46. Iwasaki A, Pillai PS. Innate immunity to influenza virus infection. Nat Rev Immunol
468 **2014**; 14:315-28.

47. Reutershan J, Vollmer I, Stark S, Wagner R, Ngamsri KC, Eltzschig HK. Adenosine and inflammation: CD39 and CD73 are critical mediators in LPS-induced PMN trafficking into the lungs. FASEB J **2009**; 23:473-82.
48. Dixit A, Cheema H, George J, Iyer S, Dudeja V, Dawra R, Saluja AK. Extracellular release of ATP promotes systemic inflammation during acute pancreatitis. Am J Physiol Gastrointest Liver Physiol **2019**; 317:G463-G75.
49. Csóka B, Németh ZH, Törő G, et al. CD39 improves survival in microbial sepsis by attenuating systemic inflammation. FASEB J **2015**; 29:25-36.
50. Aeffner F, Bratasz A, Flaño E, Powell KA, Davis IC. Postinfection A77-1726 treatment improves cardiopulmonary function in H1N1 influenza-infected mice. Am J Respir Cell Mol Biol **2012**; 47:543-51.

FIGURE LEGENDS

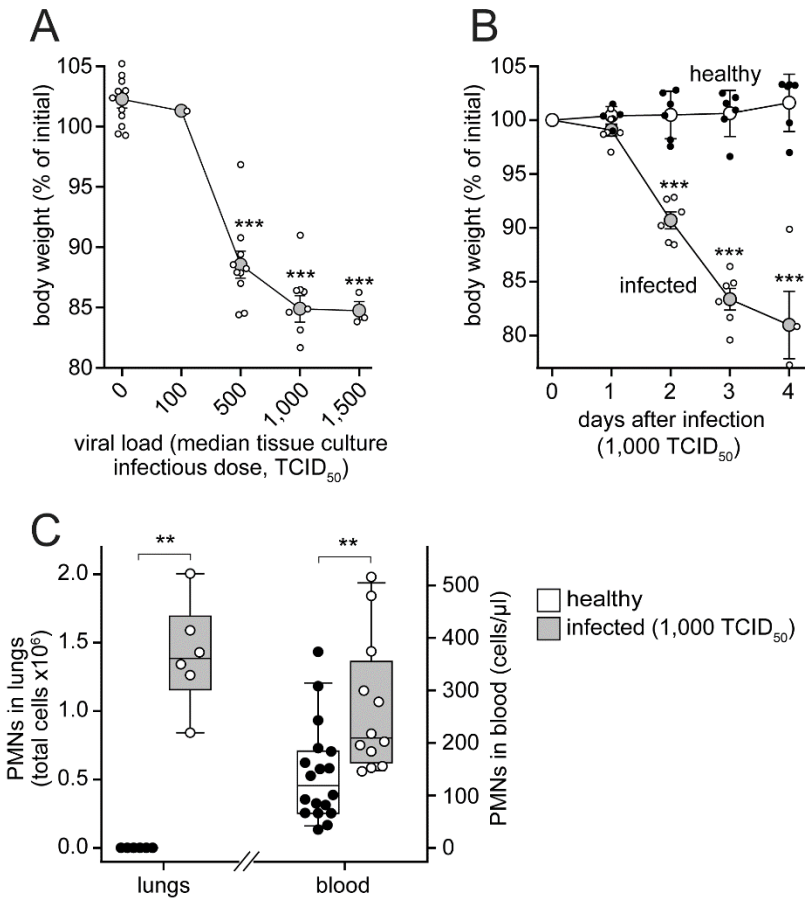

Figure 1. Influenza infection causes dose-and time-dependent weight loss and massive PMN infiltration of the lungs. A: C57BL/6J mice were intranasally infected with the indicated doses of PR8 influenza virus and body weight was measured after 3 days. Data are shown as mean ± SEM (larger circles). In panels A and B, smaller circles indicate results from individual mice; ***p<0.001 vs. uninfected controls, one-way ANOVA. **B:** Mice were infected with 1,000 $TCID_{50}$ of PR8 virus. Body weight was measured daily and compared to the weight of uninfected litter mates. Data are shown as mean ± SEM; ***p<0.001 vs. uninfected controls, t test. **C:** PMN numbers in bronchoalveolar lavage fluid (BALF) and in blood were determined 3 days after infection with 1,000 $TCID_{50}$ of PR8 virus and compared with healthy controls; **p<0.01, Mann-Whitney test.

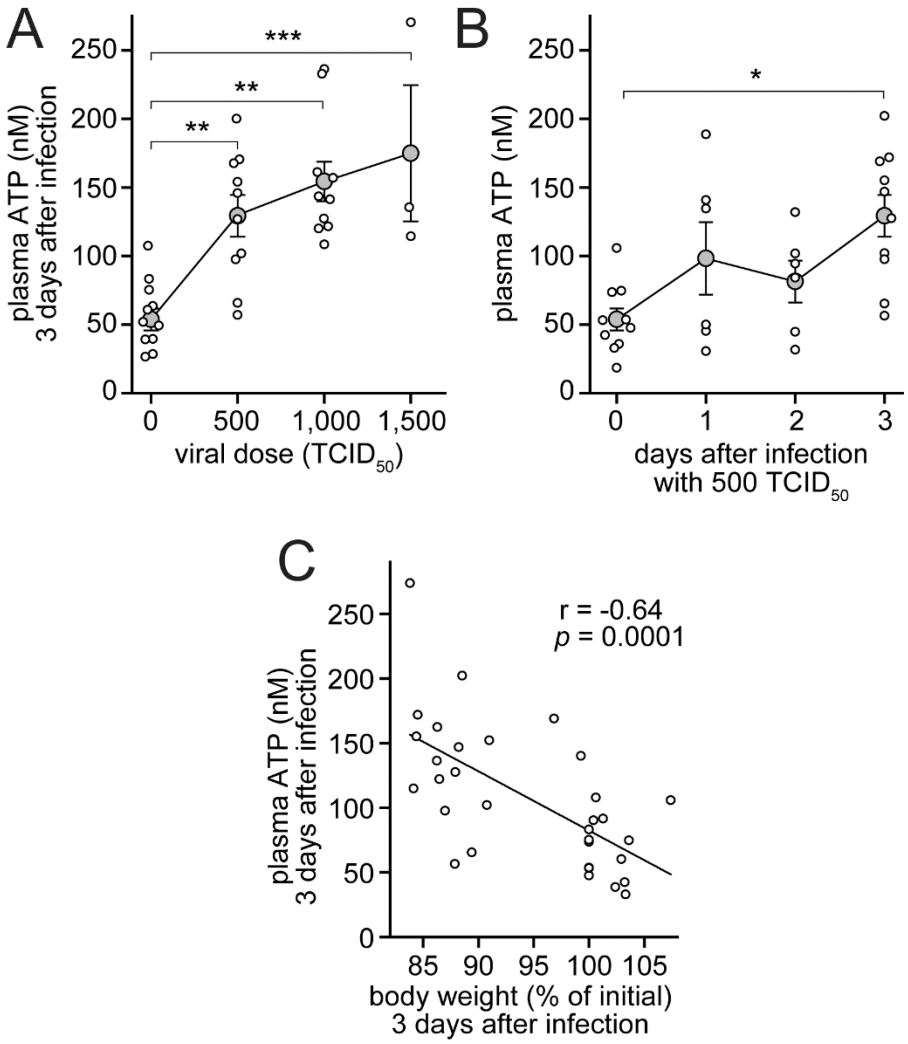

494

495 **Figure 2. Influenza elevates plasma ATP levels. A:** Mice were infected with the indicated
496 doses of PR8 influenza virus and plasma ATP levels were measured 3 days after infection.
497 Results are shown as mean ± SEM (larger circles). Smaller circles in all panels indicate results
498 from individual mice; ***p<0.001, **p<0.01, one-way ANOVA. **B:** Mice were infected with
499 500 $TCID_{50}$ of PR8 virus and ATP plasma levels were measured at indicated time points. Results
500 are shown as mean ± SEM; *p<0.05, Kruskal-Wallis test. **C:** Mice (n=30) were infected with 10-
501 1500 $TCID_{50}$ of PR8 virus and ATP plasma levels and changes in body weight were determined
502 3 days later; r: Pearson's correlation coefficient.

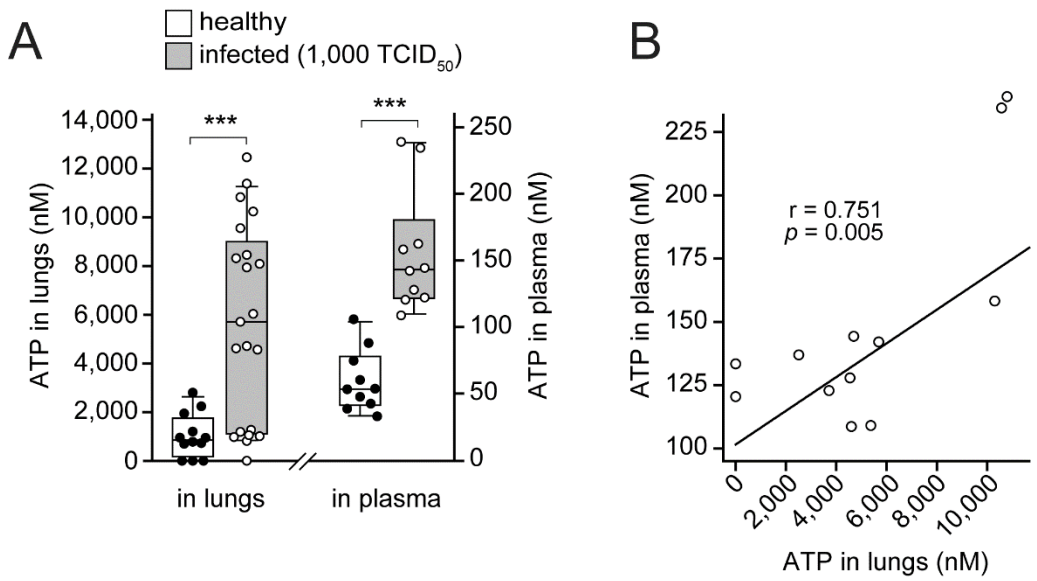

503

504 **Figure 3. Increased ATP release in the lungs of influenza-infected mice correlates with**
505 **elevated plasma ATP levels. A:** Mice were intranasally treated with PR8 virus (1,000 $TCID_{50}$)
506 or PBS (uninfected controls) and concentrations of ATP in BALF (left) and plasma (right) were
507 measured after 3 days. Circles indicate results from individual mice; ***p<0.001, Mann-Whitney
508 test. **B:** Correlation between ATP levels in plasma and alveolar fluid; r: Pearson's correlation
509 coefficient.

510

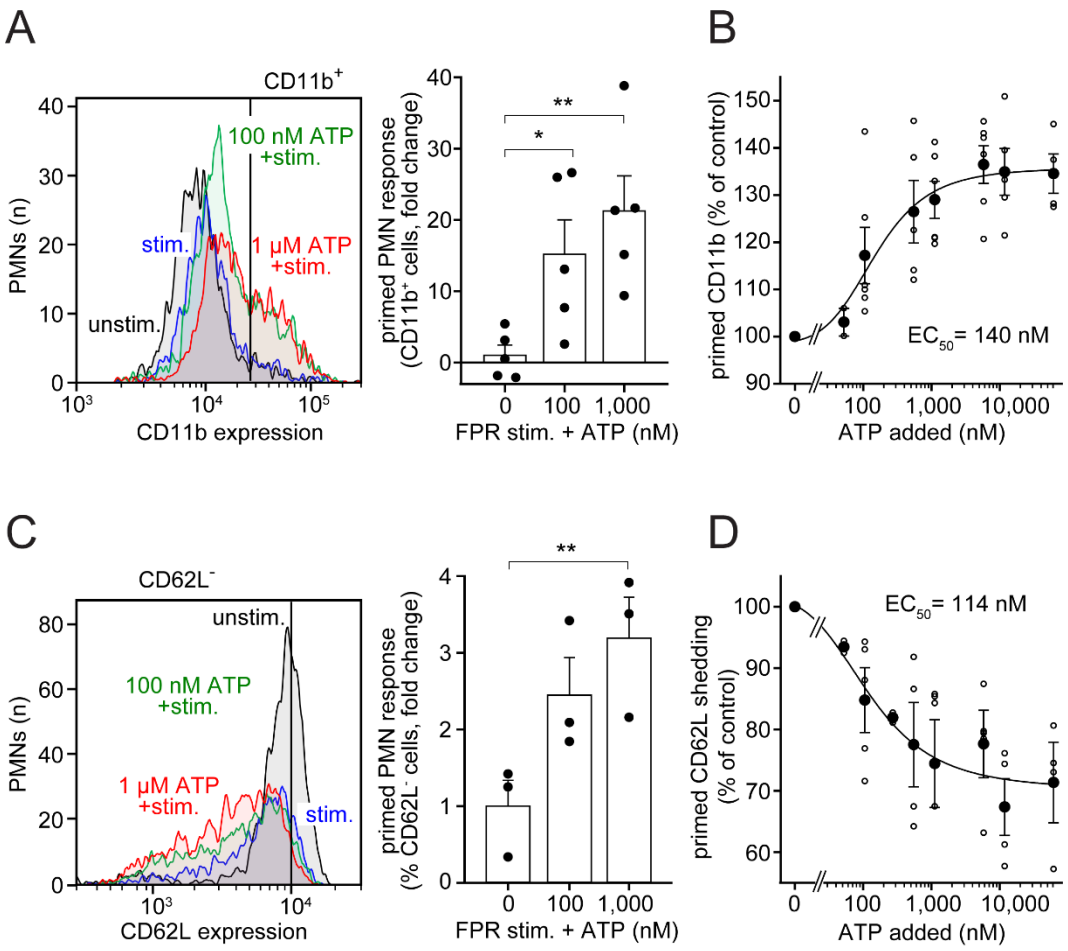

511

512 **Figure 4. Extracellular ATP primes FPR-stimulated functions of mouse PMNs.** Blood
513 samples from healthy mice were treated with the indicated concentrations of ATP and stimulated
514 with 50 nM W-peptide for 10 min and CD11b expression (**A-B**) and CD62L shedding (**B-C**)
515 were analyzed by flow cytometry. Representative histograms and means ± SEM are shown.
516 Smaller circles are data obtained with individual animals; *p<0.05, **p<0.01 vs. no ATP, one-
517 way ANOVA; EC_{50}: half maximum effective concentration; FPR: formyl peptide receptor.

518

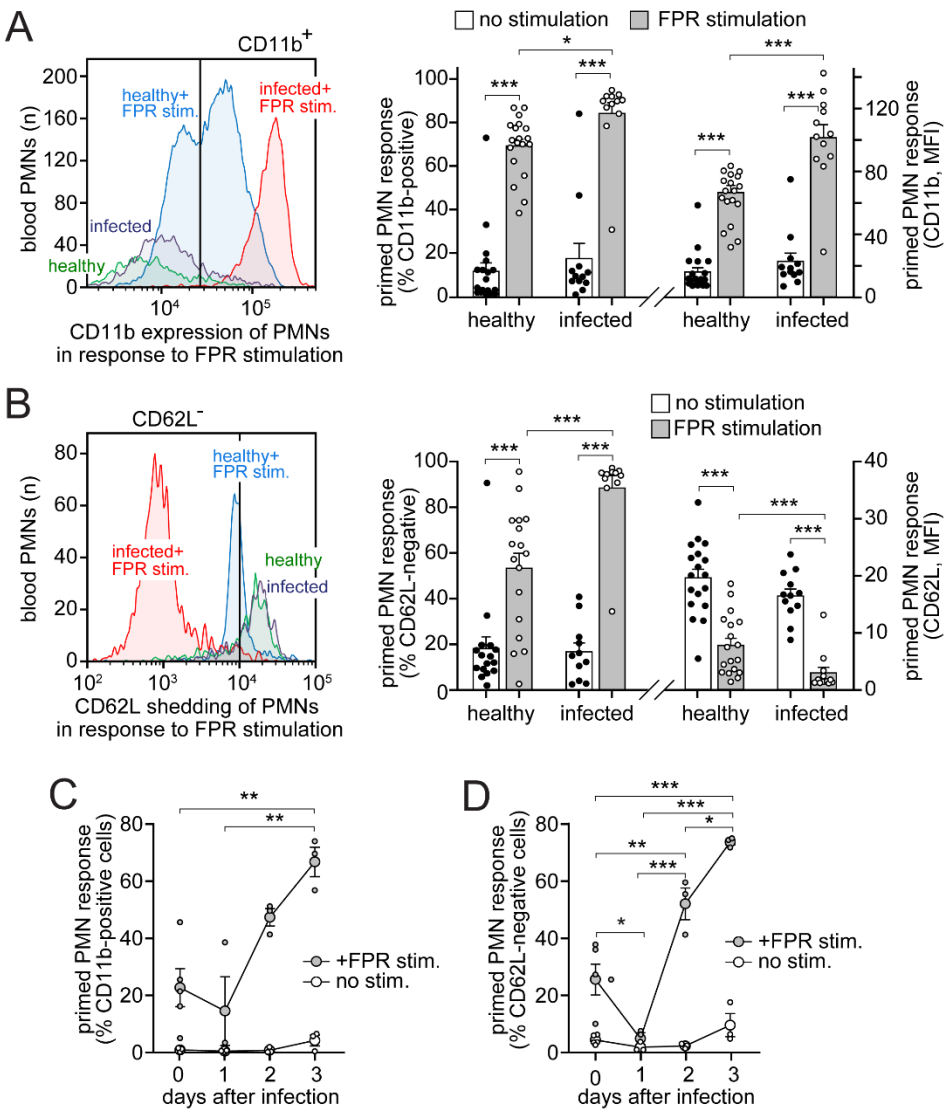

519 **Figure 5. Influenza infection primes blood PMNs.** Mice received PR8 influenza virus (1,000
520 $TCID_{50}$) or PBS (healthy control) and blood samples were collected 3 days later (**A**-**B**) or at the
521 indicated time points (**C**-**D**) and treated or not (unstimulated controls) with 100 nM W-peptide
522 for 10 min. CD11b surface expression (**A**, **C**) and CD62L shedding (**B**, **D**) were analyzed by
523 flow cytometry. Representative histograms and gating of PMN populations are shown in **A** and
524 **B**. Data are shown as mean ± SEM of at least 3 independent experiments. Circles indicate results
525 from individual mice; *p<0.05, **p<0.01, ***p<0.001, one-way ANOVA. FPR: formyl peptide
526 receptor; MFI: mean fluorescence intensity.

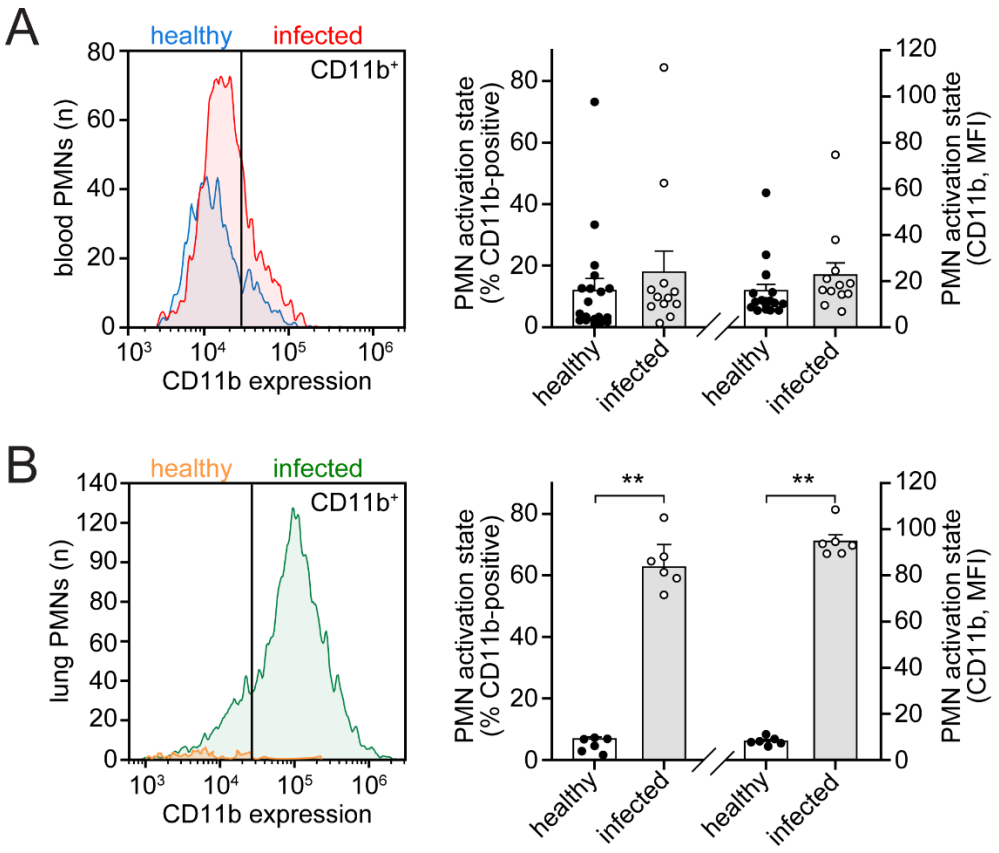

527

528 **Figure 6. Influenza virus infection activates PMNs only after their recruitment to the lungs.**

529 Mice were intranasally infected with PR8 influenza virus (1,000 $TCID_{50}$) or PBS (healthy

530 controls) and blood and BALF samples were collected 3 days later. CD11b surface expression on

531 PMNs in blood (**A**) or lungs (**B**) was analyzed by flow cytometry. Representative histograms and

532 averaged results (mean ± SEM) of at least 3 separate experiments are shown. Circles indicate

533 results from individual mice; **p=0.002, Mann-Whitney test; MFI: mean fluorescence intensity.

534

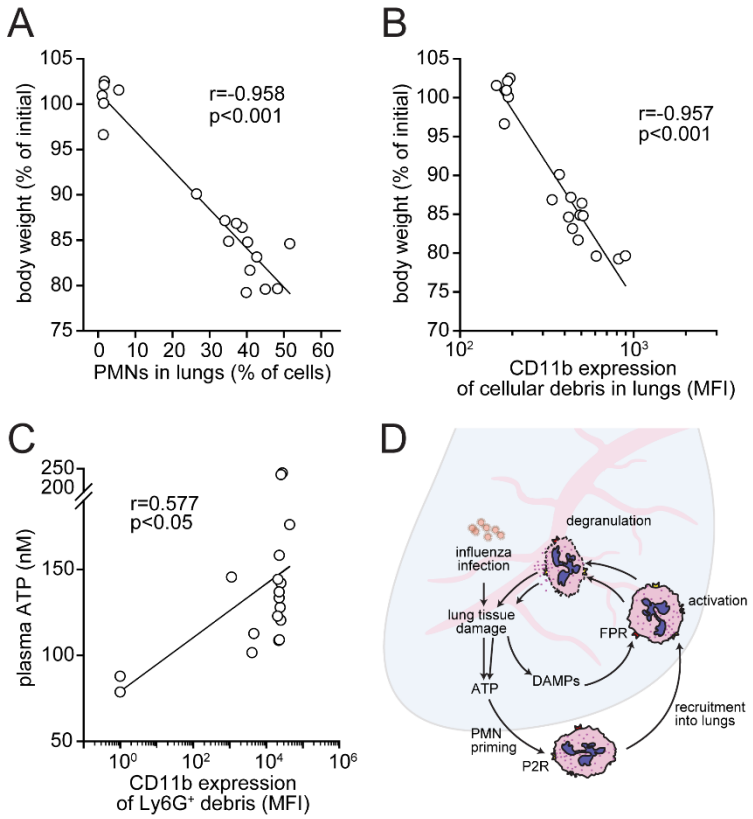

Figure 7. PMN influx correlates with disease progression. A-C: Mice received PR8 influenza virus (1,000 $TCID_{50}$; n=12) or PBS (healthy controls; n=6) and BALF samples were collected 3 days later. Samples were stained with anti-CD11b and anti-Ly6G antibodies. The percentage of PMNs (**A**) and cellular debris expressing CD11b (**B**, **C**) were analyzed by flow cytometry and correlated with body weight loss and ATP plasma levels. **D:** Proposed model of ATP-induced PMN priming and activation in influenza disease progression. Influenza-associated tissue damage releases ATP and other damage-associated molecular patterns (DAMPs) into the extracellular space. Systemic spread of ATP primes PMNs by triggering their P2 receptors (P2R). Local stimulation of primed PMNs in the lungs by FPR and DAMPs causes excessive PMN activation, degranulation, and tissue damage that promotes disease progression. FPR: formyl peptide receptor; MFI: mean fluorescence intensity

547

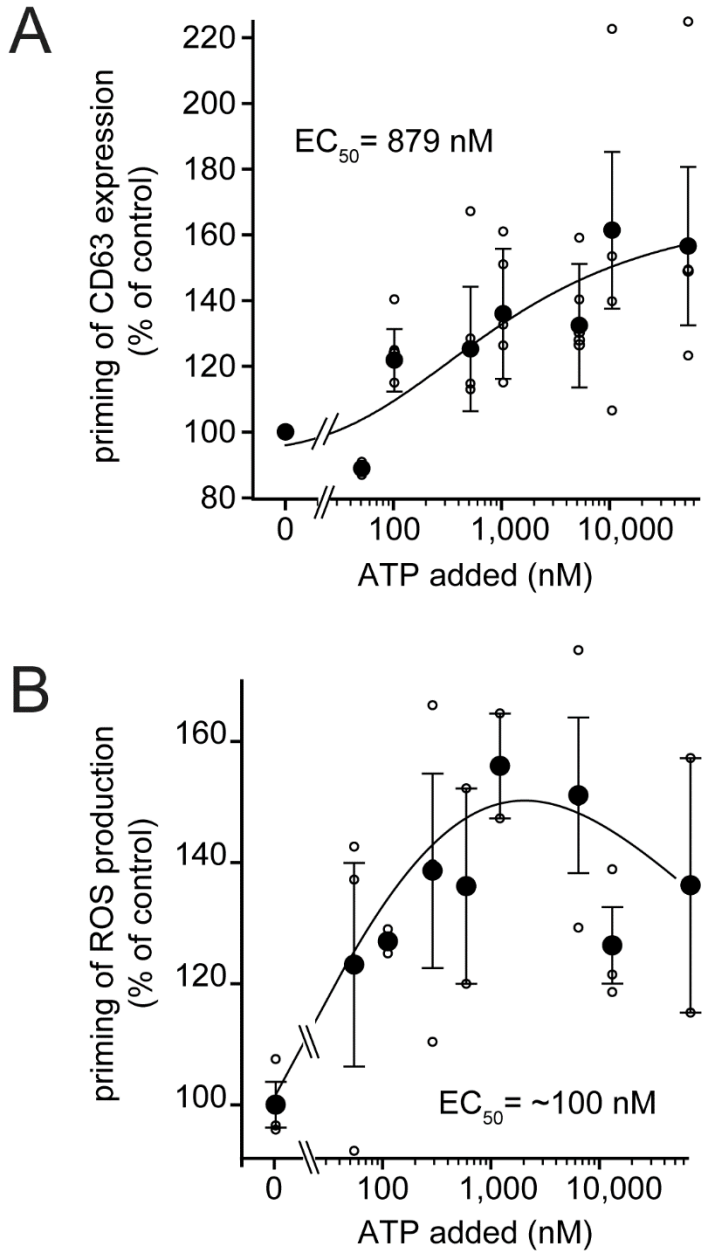

Supplementary Figure 1. Extracellular ATP primes degranulation and superoxide production of FPR-stimulated mouse PMNs. Blood samples from healthy mice were stimulated with W-peptide in the presence or absence of the indicated ATP concentrations and CD63 expression (**A**) and reactive oxygen species (ROS) production (**B**) were analyzed by flow cytometry. Results are shown as means ± SEM (n≥3 different mice); *p<0.05, **p<0.01 vs. 0 nM ATP added; one-way ANOVA; EC50: half maximum effective concentration.

548